DOI: 10.1002/chem.200800296

VIP

Hydroxycruciforms: Amine-Responsive Fluorophores

Psaras L. McGrier,[a] Kyril M. Solntsev,[a] Shaobin Miao,[a] Laren M. Tolbert,[a] Oscar R. Miranda,[b] Vincent M. Rotello,[b] and Uwe H. F. Bunz*[a]

Dedicated to Prof. Klaus Müllen

Abstract: The synthesis of three hydroxy-substituted cruciforms (XF, 1,4-bis(4′-hydroxystyryl)-2,5-bis(4″-methoxyphenylethynyl)benzene, 1,4-bis(4′-methoxystyryl)-2,5-bis(4″-hydroxyphenylethynyl)benzene, and 1,4-bis(4′-hydroxystyryl)-2,5-bis(4″-hydroxyphenylethynyl)benzene) starts with a Horner reaction followed by a Sonogashira coupling and subsequent deprotection. The three herein described XFs contain either two or four free phenolic hydroxyl groups. All three XFs were subjected to photometric UV/Vis titrations in a methanol/water mixture. The respective pK_a values were obtained by data deconvolution. As the three XFs display a significant change in emission color upon photoinduced deprotonation, the XFs were taken up in different solvents and exposed to twelve amines. The amine-dependent change in emissivity of the tetrahydroxy XF is sufficiently distinct in the eight solvents that all of the inspected amines are discerned by a linear discriminant analysis. The tetrahydroxy XF in different solvents forms a sensor array, the response of which is based on the excited-state proton transfer (ESPT) to amines and mediated by the choice of the battery of solvents that are utilized.

Keywords: alkynes · amines · fluorescence · sensors · solvatochromism

Introduction

We describe the synthesis, photophysics and amine responsive optical properties in absorption and emission of three cruciform (XF) chromophores **1**–**3**. The detection determination and quantification of low-molecular-weight amines is critical in the medical field, in environmental science, and in food safety. The enhanced presence of low-molecular-weight amines in breath can mark disease states in patients and in foods it indicates spoilage. The detection and quantification of amines has been achieved by antibodies,[1] molecularly imprinted polymers,[2] enzymes,[3] single-molecule and array sensors,[4] and chromatographic methods.[5] Recently Lavinge elegantly demonstrated that the interplay of planarization and aggregate formation in a water soluble polythiophene derivative is a powerful colorimetric tool to detect histamine in food, predicting spoilage in fish samples.[6] Inspired by Lavigne's work, we have tailored a novel class of cruciform fluorophores/chromophores (XF), 1,4-distyryl-2,5-bis(arylethynyl)benzenes, carrying phenol functionalities as model probes for amines.[7] While these small XF-fluorophores do not display aggregation or distinct planarization behavior,[8] their specifically engineered frontier molecular orbitals (FMOs) should allow signal generation and amplification of amine-probing functions such as phenols. The phenols will exhibit either full or partial proton transfer to the amine nitrogen atom, resulting in observable spectroscopic changes.

Chromophore design centers around different fundamental paradigms: 1) Choose or construct a suitable (aromatic) carbocyclic or heterocyclic skeleton, then 2) attach the necessary auxochromic groups, that is, electron-accepting or electron-releasing substituents to the skeleton to tune absorption and emission. In most chromophores donor and acceptor substituents are attached to the skeleton into positions in which both FMOs have their largest orbital nodes, ensur-

[a] P. L. McGrier, Dr. K. M. Solntsev, Dr. S. Miao, Prof. L. M. Tolbert, Prof. U. H. F. Bunz
School of Chemistry and Biochemistry
Georgia Institute of Technology, 901 Atlantic Drive
Atlanta, GA 30332-0400 (USA)
Fax: (+1) 404-385-1795
E-mail: uwe.bunz@chemistry.gatech.edu

[b] O. R. Miranda, Prof. V. M. Rotello
Department of Chemistry, 710 North Pleasant St.
University of Massachusetts, Amherst, MA 01003 (USA)

Supporting information for this article is available on the WWW under http://www.chemeurj.org/ or from the author. Experimental details are provided for the synthesis of XFs **1**–**3**, as well as details for the photophysical experiments and the absorption and emission spectra for all systems studied.

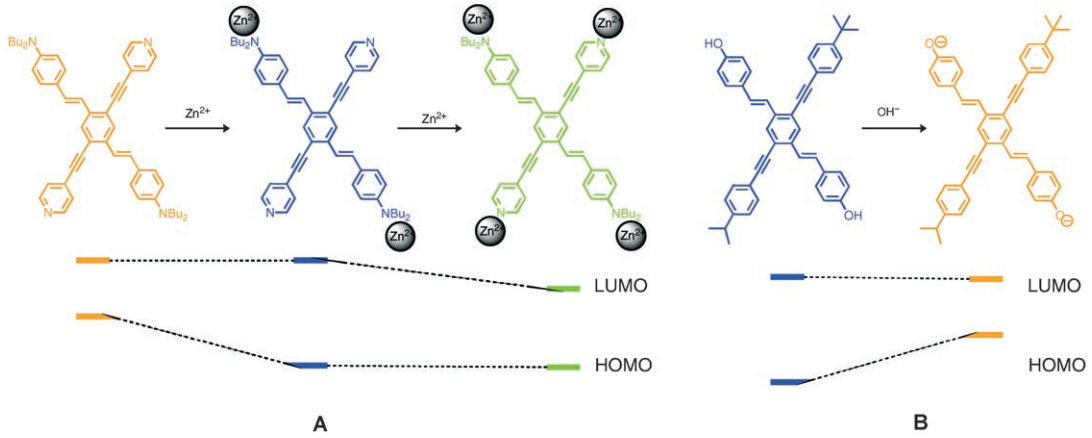

Scheme 1. Modulation of the HOMO–LUMO gap in cruciform fluorophores by interaction with metal cations and pH change.

ing the maximum conjugative effect of the auxochromes to the dye skeleton.[9] Auxochromes enlarge the π system and stabilize/destabilize both the HOMO and LUMO, but to a different degree, leading to red-shifted absorption.

We and others have designed dyes in which the geometric overlap of HOMO and LUMO is minimized. These dyes, cruciforms[10] (XF), consist of two independent but centrally connected molecular axes, which carry electron-donating and electron-withdrawing substituents respectively; this arrangement leads to a situation in which the HOMO is spatially confined on the electron-rich branch, while the LUMO is confined on the branch that carries the electron-withdrawing substituents. Examples are 1,4-distyryl-2,5-bis-(arylethynyl)benzenes,[11,12] Haley's 1,2,4,5-tetrakis(arylethynyl)benzenes,[13] Scherf's swivel cruciforms,[14] Diederich's tetraethynylethylenes,[15] and Galvin's distyrylbenzene derivatives.[16] One consequence of the spatially localized FMOs is a surprisingly large auxochromic effect; that is, absorption and emission are more strongly influenced by substituents than would be generally expected, allowing to tune the emission of a carbocyclic skeleton from blue to red. These FMO-separated phores should allow biomolecular or environmental sensing as XFs might be able to probe metal cations in cell compartments.[17] Outlined in Scheme 1 is a two-stage metalloresponsive, orange-emitting model fluorophore **A**. Upon exposure to magnesium or zinc ions the fluorescence of **A** changes to blue, but upon further increasing the amount of metal salt the fluorescence color changes from blue to yellow-green. The unusual color changes are explained by a consecutive stabilization of first the HOMO and then the LUMO of the metal-complexed XF (Scheme 1).

While we have investigated the stabilization of the FMOs, we can also induce destabilization of the HOMO by introduction of negative charges as in the hydroxy XFs **B** (Scheme 1), and indeed, deprotonation led to a red-shift in emission.[18] The LUMO of **B** is not affected according to DFT calculations. In this contribution we examine the emissive properties of three different hydroxy-substituted XFs **1**–**3** and their emissive properties upon deprotonation and upon exposure to a panel of amines in different solvents. These studies are of interest as it is possible, just by changing the solvent, to identify specific amines by the analysis of the fluorescence color of a single XF, **3**.

Results and Discussion

Synthesis: A Horner reaction of **4** with the aldehydes **5a** or **5b** furnished the distyrylbenzene derivatives **6a** and **6b** in 77 and 64% yield, respectively, after chromatography (Scheme 2). Subsequently, a Sonogashira coupling[19] with either **7a** or **7b** gave rise to the formation of **8a–c** in yields from 61 to 77%. At a temperature of −78°C trifluoroacetic acid (TFA) in dichloromethane smoothly deprotected **8a–c** to give the XFs **1**–**3** in yields around 88–92% as air and water-stable yellow powders.

Spectroscopic properties of the cruciforms 1–3: Figure 1 displays the absorption and emission spectra of **1**–**3** in different solvents (see also Tables 1–3). The spectra of tetra-ether **8c** are given for comparison. Solvatochromic behavior of **1**–**3** and **8c** was investigated.[20] Kamlet–Taft solvent parameters[21] can account for the contribution of selective (such as point-to-point hydrogen-bonding interactions) versus non-selective (solute–solvent dipole interactions) solvation to the electronic spectra of the hydroxyaromatic molecules. For **8c** the absorbance spectra depend weakly on solvent polarity, indicating a small ground-state dipole moment. The emission spectra of **8c** exhibit stronger bathochromic shifts in polar solvents due to the increase in dipole moment upon excitation (Table 4). All four compounds (**8c**, **1**–**3**) are isoelectronic. We assume that their dipole moments in the ground and the excited states are similar. Therefore, additional bathochromic shifts in the di- and tetrahydroxy cruciforms are related to hydrogen-bonding between the hydroxy groups of the chromophores and basic solvents, such as DMSO or DMF. However, these shifts are small, indicating weak acidity of phenol moieties in both ground and excited states. A weak shoulder located at 530 nm in the emission of

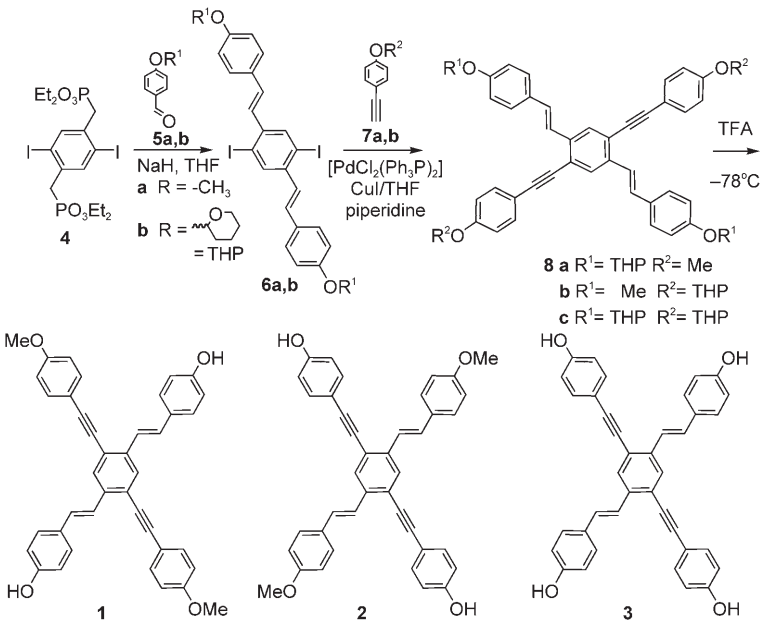

Scheme 2. Synthesis of cruciforms **1**–**3** by a combination of Horner and Sonogashira methods.

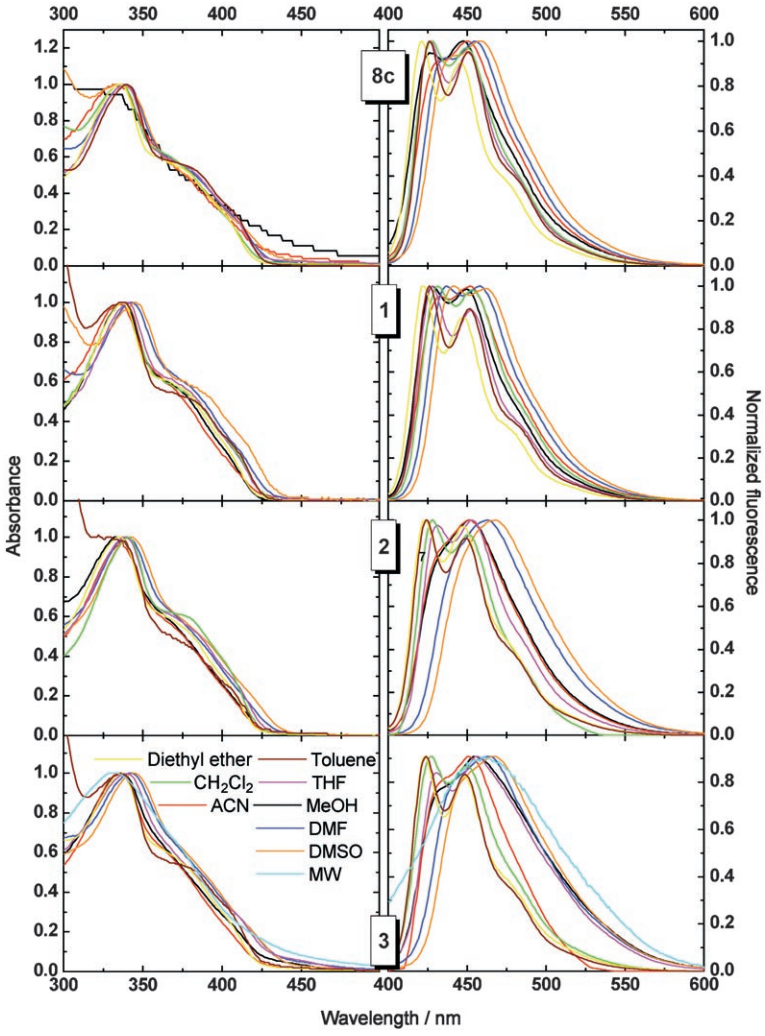

Figure 1. Absorption and emission spectra of **8c** and **1**–**3** in different solvents. The color coding is the identical for all graphs. MW is 1:9 vol. methanol/water.

3 in 90% water/methanol solvent mixture might be associated with the excited-state proton-transfer product.[22] For all dyes the fluorescence quantum yield (Φ) in methanol was in the range of 16–37% (Table 5). Compound **2** has the highest quantum yield and the longest emissive lifetime (τ = 1.6 ns). It is not clear what the reason is for the differences in the structurally similar XFs.

The compounds **1** and **2** were poorly soluble in pure water at neutral pH, demonstrating formation of red-shifted aggregates in the absorbance spectra (see Supporting Information). A comparative study of the acid–base behavior of **1**–**3** was performed in a 2:1 volume ratio of methanol/water (Figure 2). However, the absorbance spectra of **2** in this solvent at neutral pH differed from that in various organic solvents. Thus, the absorbance titration data of **2** should be evaluated with caution, since it reflects not only deprotonation, but also the dissolution of its aggregates. This aggregation phenomenon at neutral pH is observed also for **1**, but to a much lesser extent. The three compounds respond differently towards hydroxide ions in absorption and emission. In the case of **1** a new band emerges (416 nm, UV/Vis), which is fully developed at pH 12. Visually, the almost colorless solution turns yellow. Simultaneously, a new band at 600 nm appears in the emission spectra, similar to that described by us for **B** (Scheme 1), while the emission at 460 nm dissapears due to full ground-state deprotonation. At higher pH the long-wavelength emission exhibits a small hypsochromic shift. The titration of XF **2** did not lead to the formation of the characteristic red-shifted phenolate band in the absorbance spectra, and the fluores-

Table 1. Absorption and emission maxima for **1** in different solvents.

Solvent	$\lambda_{max\,abs}$ [nm]	$\lambda_{max\,em}$ [nm]	Stokes shift [cm^{-1}]	Vibronic progression [cm^{-1}]
methanol	336, 365 sh	451	7589, 5224	-
acetonitrile	337, 370 sh	451	7501, 4854	-
DMF	340, 375 sh	463	7813, 5068	-
DMSO	343, 380 sh	468	7787, 4948	-
THF	339, 370 sh	431, 453	6297, 3825	1127
CH_2Cl_2	342, 380 sh	428, 451	5875, 2951	1192
diethyl ether	336, 370 sh	423, 447	6121, 3386	1269
toluene	339, 375 sh	424, 449	5914, 3082	1313

Table 2. Absorption and emission maxima for **2** in different solvents.

Solvent	$\lambda_{max\,abs}$ [nm]	$\lambda_{max\,em}$ [nm]	Stokes shift [cm^{-1}]	Vibronic progression [cm^{-1}]
methanol	338, 370 sh	428, 450	6221, 3663	1142
acetonitrile	337, 370 sh	433, 452	6579, 3932	971
DMF	344, 375 sh	437, 458	6186, 3783	1049
DMSO	346, 380 sh	441, 462	6226, 3640	1031
THF	341, 370 sh	428, 453	5961, 3663	1289
CH_2Cl_2	339, 375 sh	431, 453	6297, 3465	1127
diethyl ether	338, 370 sh	422, 448	5889, 3330	1375
toluene	339, 380 sh	426, 452	6024, 2842	1350

Table 3. Absorption and emission maxima for **3** in different solvents.

Solvent	$\lambda_{max\,abs}$ [nm]	$\lambda_{max\,em}$ [nm]	Stokes shift [cm^{-1}]	Vibronic progression [cm^{-1}]
90:10 H_3C–OH/H_2O	334	458	8106	-
methanol	337	435, 456	6685	1059
acetonitrile	335	438, 450	7020	609
DMF	343	464	7602	-
DMSO	345	467	7572	-
THF	340	432, 456	6264	1218
CH_2Cl_2	332	428, 450	6756	1142
diethyl ther	337, 370 sh	424, 449	6089, 3442	1313
toluene	336	424, 448	6177	1263

Table 4. Absorption and emission maxima for **8c** in different solvents.

Solvent	$\lambda_{max\,abs}$ [nm]	$\lambda_{max\,em}$ [nm]	Stokes shift [cm^{-1}]	Vibronic progression [cm^{-1}]
methanol	insoluble	427, 448	–	–
acetonitrile	331, 370 sh	433, 451	7116, 4854	922
DMF	338, 385 sh	436, 455	6650, 4689	958
DMSO	332, 370 sh	441, 458	7445, 5193	842
THF	338, 375 sh	427, 451	6167, 4494	1246
CH_2Cl_2	336, 370 sh	428, 450	6397, 4805	1142
diethyl ether	335, 375 sh	421, 446	6098, 4245	1331
toluene	340, 380 sh	426, 451	5938, 4143	1301

Table 5. Photophysical data of **1**–**3** in methanol.

	1	**2**	**3**
Abs [nm]	336, 365	338, 370	337
Em [nm]	433, 451	430, 451	435, 456
Φ	0.17	0.37	0.16
τ [ns]	0.80	1.60	0.89

cence spectra were quenched without appearance of a new low-energy band. Similar effects were observed by us earlier[18] for some other dihydroxycruciforms. On the basis of MO calculations we have demonstrated that the HOMO and LUMO orbitals of such molecules have a vanishing overlap, which makes the S_0–S_1 electronic transition forbidden. As a result, bathochromic shifts in the absorbance spectra were not observed upon deprotonation; the emission from the deprotonated species is so weak that it can not be recorded. The XF **3**, with four hydroxy groups, features a diffuse isosbestic point around 346 nm; upon deprotonation a prominent feature develops at 370 nm. We assumed that the terminal spectra at the highest pH value for each XF belong to the fully deprotonated form of the respective chromophore. The absorbance spectra of the tetra-anion of **3** can be viewed as a superposition of **1** and **2** dianion bands. To understand these effects, we analyzed the photometric absorption data using the SPECFIT software.[22b] Figure 3 displays the relative amounts of the corresponding deprotonated species present and the deconvoluted spectra of the neutral compound and all of the phenolate anions up to the tetra-anion for **3**.

Upon increasing the pH the absorption profiles of the formed mono-, di-, tri-, and tetra-anion are deconvoluted. Their absorption maximum is consecutively red-shifted from 335 to 370 nm.

When traversing from pH 7 to pH 10 we observe a significantly red-shifted (588 nm) emission band of lower intensity in **3**. Upon further increase of the pH, the fluorescence intensity of **3** increases again and the emission maximum blue-shifts to 565 nm. The results of the fit demonstrate the coexistence of several polyanions of **3** at different pH regimes. It is surprising that in contrast to polyphenols[23] the pK_a's of four hydroxyl groups differ by not more than one unit. A possible explanation for this phenomenon is the weak electronic interaction between two pairs of hydroxyls located on the distyrylbenzene and arylethynyl axes of the molecules. Another important observation from the data fitting is the pH mismatch in the existence areas of the different acid–base species for the ground- and the excited-state titrations. Such spectral behavior is a classical example of the photoacidity in the hydroxyaromatic molecules.[24] We note, though, that the apparent shifts between the ground- and excited-state pK_a's are only about one unit, demonstrating a small but detectable increase of the photoacidity in aqueous solutions.

Amine sensing using the cruciforms 1–3: With these results in hand we set out to explore the fluorescence change of the XFs **1**–**3** upon exposure towards different amines. We prepared 10 μM solutions of the respective XFs in eight different solvents. These were then distributed into 13 vials each to obtain a matrix of 12 amines plus reference in 8 solvents to give 104 samples per XF. The amine (0.1 mL per sample, an excess, corresponding to a 0.7–7.2 mM concentration range) was then added and a picture of the 13 samples with 12 different amines for each of the eight solvents was taken

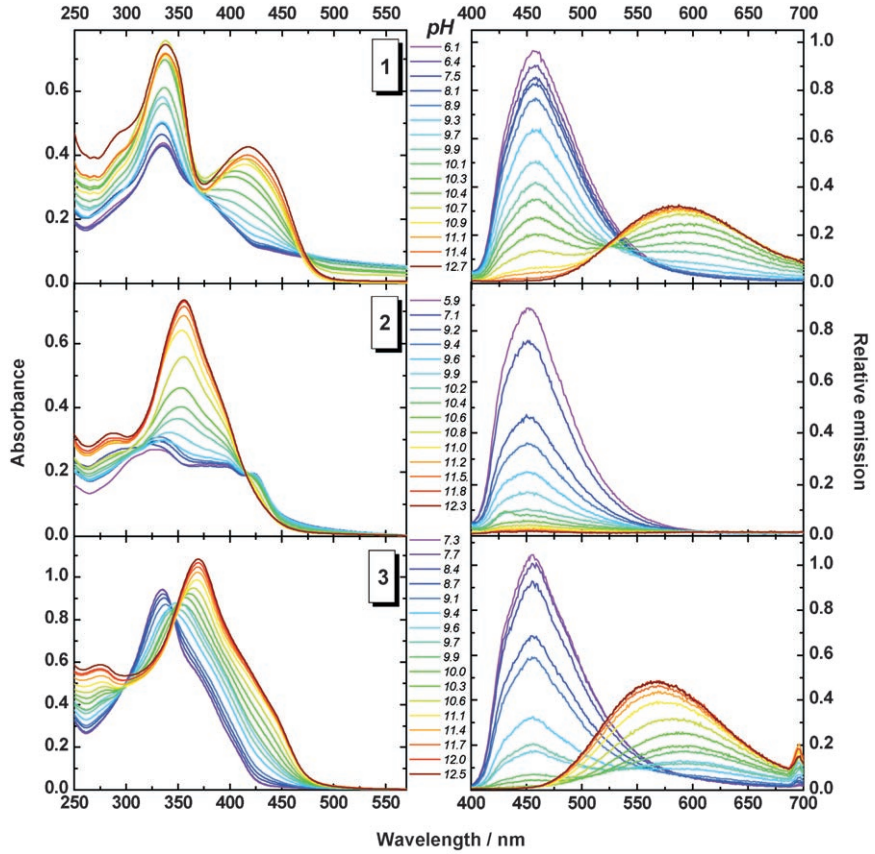

Figure 2. Absorption and emission spectra of **1**–**3** in 2:1 vol. methanol/water mixtures at different pH. The band at 690 nm in the emission titration of **3** is a scattering peak and represents double the excitation wavelength.

While the XF **1** gives color changes in emission, the XF **2** mostly experiences quenching (see the Supporting Information), similar to the titration in a methanol/water mixture. The XF **3**, however, experienced spectacular changes in fluorescence upon the combination of amines, with the emission colors ranging from blue to red traversing yellow and green, covering the full visible spectral range.

Ground- and excited-state acid–base interactions between dihydroxycruciforms and various amines in dichloromethane were studied[18] and the fluorophores exhibit emission from the fully deprotonated (ion pair) state. From these observations we concluded that in dichloromethane the difference in pK_a (or ΔG of the proton transfer) between the excited dihydroxycruciforms and amines is sufficient to produce the solvent-separated ion pair with the emission around 550 nm.[25] In the ground state the observed ΔpK_a results in the formation of the hydrogen-bonded complexes.

(Figure 4). These real-color photographs were taken in the dark upon irradiation with a hand-held UV-lamp at an emission wavelength of 366 nm.

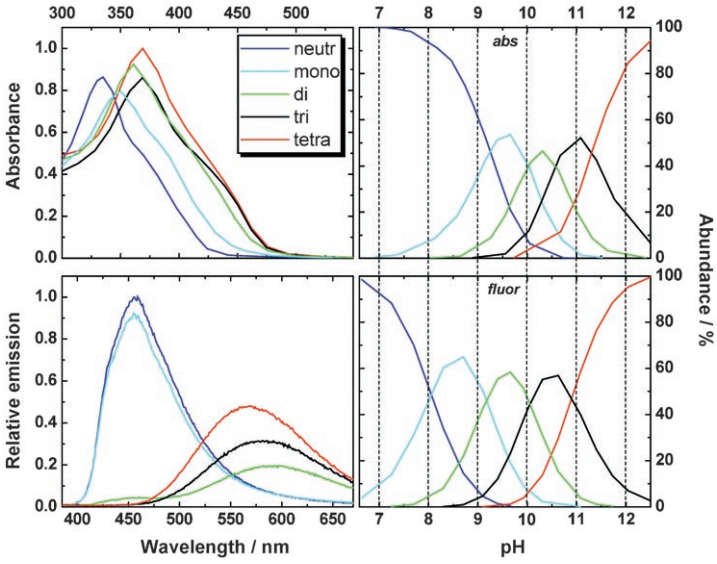

Figure 3. Deconvoluted absorption and emission spectra of the anions of **3** with relative pK_a values: $pK_{a1}=9.2(\pm0.1)$; $pK_{a2}=10.0(\pm0.2)$; $pK_{a3}=10.6(\pm0.3)$; $pK_{a4}=11.3(\pm0.2)$.

Generally, a similar behavior of **1** and **3** is observed in the present work for an array of solvents and amines. The only amine that quantitatively deprotonates the XFs in the ground state is the most basic DBU; significant changes occur both in absorption as well as in emission (Figure 5). While only DBU leads to a significant shift in absorption, almost all amines lead to a red-shift in the emission of **3**.

We were successful in utilizing the Kamlet–Taft method[21] to analyze the solvatochromic behavior of the ESPT product emission maxima, that is, the vertical columns in Figure 4. For instance, for **3** the solvent dependence of the emission maxima (ν) of the long-wavelength band in the presence of ethylenediamine can be presented as Equation (1):

$$\nu(10^3\ \mathrm{cm}^{-1}) = 19.8 - 2.7\pi^* - 0.9\beta + 0.7\alpha \quad (r = 0.95) \tag{1}$$

in which π^*, β, and α are Kamlet–Taft solvent parameters reflecting the polarity, basicity, and acidity, respectively, of the solvent (r = residual). From this analysis one can see that the increase of solvent polarity and basicity causes the bathochromic shift of the emission, while the acidity of the solvent works in opposite direction. The magnitudes of the co-

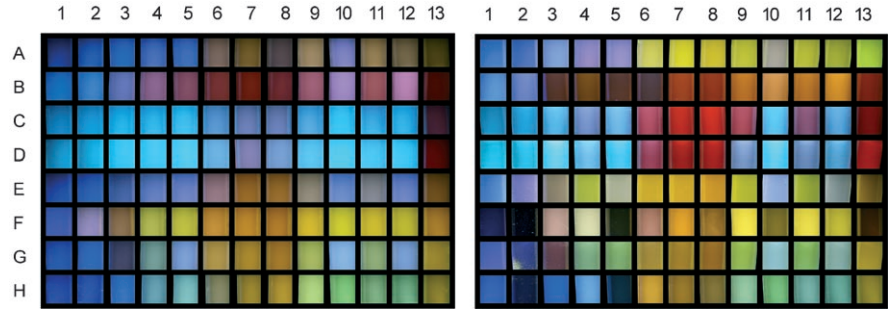

Figure 4. Photographs of solutions of **1** (left), and **3** (right) upon addition of amines 2–13 (left to right) 1) XF reference, 2) histamine (6.9), 3) imidazole (6.9), 4) morpholine (8.3), 5) piperazine (9.8), 6) putrescine (9.9), 7) 1,3-diaminopropane (10.5), 8) ethylenediamine (10.7), 9) piperidine (10.8), 10) triethylamine (10.8), 11) diethylamine (11.0), 12) diisopropylamine (11.1), 13) 1,8-diazabicyclo[5.4.0]undec-7-ene (DBU ≈12) [numbers in parentheses are the pK_a values of the corresponding ammonium ions in water] in different solvents (top to bottom): A) methanol, B) acetonitrile, C) DMF, D) DMSO, E) THF, F) dichloromethane, G) diethyl ether, and H) toluene. The samples were excited by using a hand-held UV-lamp at an emission wavelength of 366 nm.

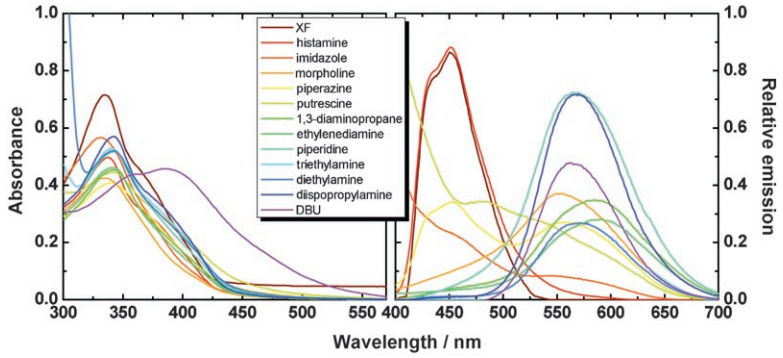

Figure 5. Absorption and emission of XF **3** in acetonitrile upon addition of different amines. Note that only DBU gives a significant red shift in absorption, while almost all amines give a significant shift in emission.

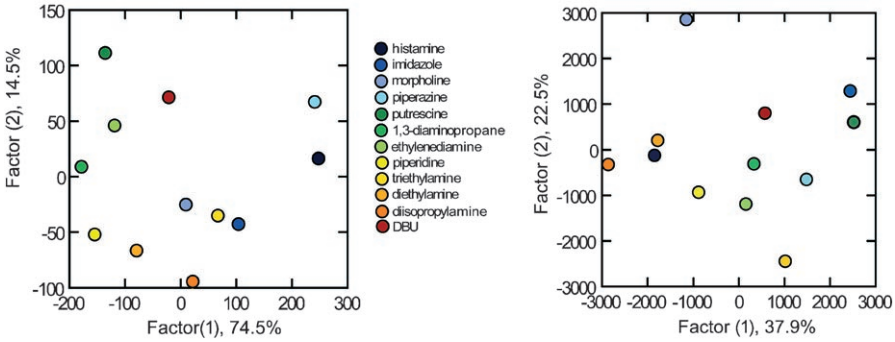

Figure 6. Linear discriminant analysis (LDA) of the differential RGB values (left) and ratio intensities (right) of **3** obtained from the right-hand side of Figure 4. The data on the left were extracted from the matrix generated by the RGB values measured for the photographs of the XF **3** dissolved in eight solvents in the presence of each different amine. The data on the right were extracted from the λ_{max} of emission and the relative fluorescence intensities of **3** in the presence of each amine. All of the amines are separated in the 2D LDA-plot. The two factors do not represent a specific chemical property of the amines, such as pK_a value, chemical structure or other evident chemical properties in either case.

efficients demonstrate the dominating role of the polarity in the solvatochromic behavior of the fluorescence. Interestingly, the data from the horizontal rows in Figure 4 (emission maxima) did not have a straightforward correlation with the pK_a.

While the photographs give a good indication to discern 12 amines by **3**, we converted the color into RGB values and subtracted the RGB value of the reference using the program Contrast Analyzer.[26] Two independent readings yielded RGB values for the XF **3** that were subjected to an LDA analysis with the program SYSTAT (Figure 6).[27] With 24 different data points for each amine, SYSTAT reduces the data into a 2D LDA plot containing only two factors. The 12 amines are cleanly separated according to the analysis of their RGB values, allowing us to discern diethylamine and triethylamine or diethylamine and diisopropylamine. Interestingly, the amines are not grouped in this LDA plot according to their pK_a values; however, the diamines (green) with exception of piperazine are grouped together, and secondary amines such as piperidine, diethylamine, and diisopropylamine (yellow-orange) are also grouped together at the bottom of the plot.

Conclusion

In conclusion, we have synthesized three phenolic XFs **1**–**3**. XFs **1** and **3** display red-shifted absorption and emission upon deprotonation in methanol/water mixtures and were investigated for amine sensing. A series of 12 different amines could be discerned by the specific fluorescence response of **3** based on excited-state proton transfer in eight different solvents. These experiments imply that one can create a "chemical nose" by using only one sensor molecule, but in different environments, that is, solvents. The emission wavelength of XF **3** is exquisitely sensitive towards different amines, and

that in a solvent dependent fashion. The selectivity and responsivity of one fluorophore suffices to constitute a small sensor array just by changing the solvent. Using solutions of **3** would not be the most effective way to design a strip sensor or a similar application-oriented gadget, but the proof of principle is important, as XFs could easily be incorporated into grafted, conjugated polymers, in which the appended, non-conjugated polymer chains should be able to substitute for the solvent. Such materials could be spin cast onto silanized silica gel and their color response be observed upon exposure towards amines in air or water. The herein described experiments serve as a valuable guide for the design and execution of such polymeric materials, upon which we will report in the future. The colorful hydroxy XFs **1** and **3** display large and unique ratiometric shifts upon exposure to amines and are fascinating objects, fit for further evaluation exploiting the principles of spatial separation of FMOs and the mechanisms of the photoinduced proton transfer.

Experimental Section

The experimental details for the synthesis of XFs **1–3**, as well as details for the photophysical experiments and the absorption and emission spectra for all systems studied are available in the Supporting Information.

Acknowledgements

We thank the National Science Foundation for financial support (CHE-0456892 for K.S. and L.T., CHE-0750275 for U.B. and P.M.), Prof. Christoph Fahrni for helpful discussions and Prof. Rob Dickson for the use of the CAROM lifetime spectroscopy setup. P.M. thanks The Georgia Institute of Technology for a FACES fellowship. The authors thank Katja Kouznetsova for help with the cover.

[1] Z. M. Merchant, S. G. G. Cheng, in *Characterization of Foods: Emerging Methods* (Ed.: A. G. Gaonkar), Elsevier Science, New York, **1995**, Chapter 15.

[2] a) N. T. Greene, K. D. Shimizu, *J. Am. Chem. Soc.* **2005**, *127*, 5695–5700; b) E. Mertz, S. C. Zimmerman, *J. Am. Chem. Soc.* **2003**, *125*, 3424–3425.

[3] C. Yeh, S. Lin, D. Hwang, *J. Food Drug Anal.* **2004**, *12*, 128–132.

[4] a) N. A. Rakow, A. Sen, M. C. Janzen, J. B. Ponder, K. S. Suslick, *Angew. Chem.* **2005**, *117*, 4604–4608; *Angew. Chem. Int. Ed.* **2005**, *44*, 4528–4532; b) K. S. Suslick, N. A. Rakow, A. Sen, *Tetrahedron* **2004**, *60*, 11133–11138; c) N. A. Rakow, K. S. Suslick, *Nature* **2000**, *406*, 710–713; d) M. S. Freund, N. S. Lewis, *Proc. Natl. Acad. Sci. USA* **1995**, *92*, 2652–2656; e) A. T. Wright, E. V. Anslyn, *Chem. Soc. Rev.* **2006**, *35*, 14–28; f) Y. Vlasov, A. Legin, A. Rudnitskaya, *Pure Appl. Chem.* **2005**, *77*, 1965–1983; g) A. Deisingh, K. Stone, D. C. Thompson, M. *Int. J. Food Sci. Tech.* **2004**, *39*, 587–604; h) J. J. Lavigne, E. V. Anslyn, *Angew. Chem.* **2001**, *113*, 3212–3225; *Angew. Chem. Int. Ed.* **2001**, *40*, 3118–3130.

[5] a) S. Rossi, C. Lee, P. C. Ellis, L. F. Pivarnlik, *J. Food Sci.* **2002**, *67*, 2056–2060; b) C. Ruiz-Capillas, A. Moral, *J. Food Sci.* **2001**, *66*, 1030–1032; c) A. H. Ritchie, I. M. Mackie, in *Advances in Fish Science and Technology* (Ed.: J. J. Connell), Fishing News, Farnham (UK), **1980** pp. 489–494.

[6] a) T. L. Nelson, I. Tran, T. G. Ingallinera, M. S. Maynor, J. J. Lavigne, *Analyst* **2007**, *132*, 1024–1030; b) M. S. Maynor, T. L. Nelson, C. O'Sullivan, J. J. Lavigne, *Org. Lett.* **2007**, *9*, 3217–3220; c) T. L. Nelson, C. O'Sullivan, N. T. Greene, M. S. Maynor, J. J. Lavigne, *J. Am. Chem. Soc.* **2006**, *128*, 5640–5641.

[7] J. N. Wilson, M. Josowicz, Y. Q. Wang, U. H. F. Bunz, *Chem. Commun.* **2003**, 2962–2963.

[8] a) C. E. Halkyard, M. E. Rampey, L. Kloppenburg, S. L. Studer-Martinez, U. H. F. Bunz, *Macromolecules* **1998**, *31*, 8655–8659; b) J. Kim, T. M. Swager, *Nature* **2001**, *411*, 1030–1034.

[9] H. Zollinger, *Color Chemistry*, 3rd ed., Wiley-VCH, Weinheim (Germany), **2003**.

[10] For the first use of the term cruciforms for dyes see: J. E. Klare, G. S. Tulevski, K. Sugo, A. de Picciotto, K. A. White, C. Nuckolls, *J. Am. Chem. Soc.* **2003**, *125*, 6030–6031.

[11] a) J. N. Wilson, U. H. F. Bunz, *J. Am. Chem. Soc.* **2005**, *127*, 4124–4125; b) W. W. Gerhardt, A. J. Zucchero, J. N. Wilson, C. R. South, U. H. F. Bunz, M. Weck, *Chem. Commun.* **2006**, 2141–2143; c) A. J. Zucchero, J. N. Wilson, U. H. F. Bunz, *J. Am. Chem. Soc.* **2006**, *128*, 11872–11881.

[12] a) J. Tolosa, E. Diez-Barra, P. Sanchez-Verdu, J. Rodriguez-Lopez, *Tetrahedron Lett.* **2006**, *47*, 4647–4651; b) J. K. Sorensen, M. Vestergaard, A. Kadziola, K. Kilsa, M. B. Nielsen, *Org. Lett.* **2006**, *8*, 1173–1176; c) S. Grunder, R. Huber, V. Horhoiu, M. T. Gonzalez, C. Schonenberger, M. Calame, M. Mayor, *J. Org. Chem.* **2007**, *72*, 8337–8344; d) K. Hu, P. W. Zhu, Y. Yu, A. Facchetti, T. J. Marks, *J. Am. Chem. Soc.* **2004**, *126*, 15974–15975.

[13] a) J. A. Marsden, J. J. Miller, L. D. Shirtcliff, M. M. Haley, *J. Am. Chem. Soc.* **2005**, *127*, 2464–2476; b) J. A. Marsden, M. M. Haley, *J. Org. Chem.* **2005**, *70*, 10213–10226; c) J. A. Marsden, J. J. Miller, M. M. Haley, *Angew. Chem.* **2004**, *116*, 1726–1729; *Angew. Chem. Int. Ed.* **2004**, *43*, 1694–1697.

[14] a) A. Zen, A. Bilge, F. Galbrecht, R. Alle, K. Meerholz, J. Grenzer, D. Neher, U. Scherf, T. Farrell, *J. Am. Chem. Soc.* **2006**, *128*, 3914–3915; b) A. Bilge, A. Zen, M. Forster, H. B. Li, F. Galbrecht, B. S. Nehls, T. Farrell, D. Neher, U. Scherf, *J. Mater. Chem.* **2006**, *16*, 3177–3182

[15] a) L. Gobbi, P. Seiler, F. Diederich, *Angew. Chem.* **1999**, *111*, 737–740; *Angew. Chem. Int. Ed.* **1999**, *38*, 674–678; b) F. Diederich, *Chem. Commun.* **2001**, 219–227; c) R. R. Tykwinski, U. Gubler, R. E. Martin, F. Diederich, C. Bosshard, P. Gunter, *J. Phys. Chem. B* **1998**, *102*, 4451–4465; d) R. R. Tykwinski, M. Schreiber, R. P. Carlon, F. Diederich, V. Gramlich, *Helv. Chim. Acta* **1996**, *79*, 2249–2281; e) A. Hilger, J. P. Gisselbrecht, R. R. Tykwinski, C. Boudon, M. Schreiber, R. Martin, H. P. Lüthi, M. Gross, F. Diederich, *J. Am. Chem. Soc.* **1997**, *119*, 2069–2078; f) F. Mitzel, C. Boudon, J. P. Gisselbrecht, P. Seiler, M. Gross, F. Diederich, *Helv. Chim. Acta* **2004**, *87*, 1130–1157; g) J. P. Gisselbrecht, N. N. P. Moonen, C. Boudon, M. B. Nielsen, F. Diederich, M. Gross, *Eur. J. Org. Chem.* **2004**, 2959–2972.

[16] Z. I. Niazimbetova, H. Y. Christian, Y. J. Bhandari, F. L. Beyer, M. E. Galvin, *J. Phys. Chem. A* **2004**, *108*, 8673–8681.

[17] a) M. M. Henary, Y. G. Wu, C. J. Fahrni, *Chem. Eur. J.* **2004**, *10*, 3015–3025; b) B. Wang, M. R. Wasielewski, *J. Am. Chem. Soc.* **1997**, *119*, 12–21; c) C. G. Bangcuyo, M. E. Rampey-Vaughn, L. T. Quan, S. M. Angel, M. D. Smith, U. H. F. Bunz, *Macromolecules* **2002**, *35*, 1563–1568; d) T. Pautzsch, E. Klemm, *Macromolecules* **2002**, *35*, 1569–1575; e) S. J. K. Pond, O. Tsutsumi, M. Rumi, O. Kwon, E. Zojer, J. L. Bredas, S. R. Marder, J. W. Perry, *J. Am. Chem. Soc.* **2004**, *126*, 9291–9306; f) L. C. Yang, R. McRae, M. M. Henary, R. Patel, B. Lai, S. Vogt, C. J. Fahrni, *Proc. Natl. Acad. Sci. USA* **2005**, *102*, 11179–11184; g) J. Cody, C. J. Fahrni, *Tetrahedron* **2004**, *60*, 11099–11107; h) R. Corradini, A. Dossena, G. Galaverna, R. Marchelli, A. Panagia, G. Sartor, *J. Org. Chem.* **1997**, *62*, 6283–6289; i) S. W. Thomas III, G. D. Joly, D. Guy, T. M. Swager, *Chem. Rev.* **2007**, *107*, 1339–1386; j) A. Ono, H. Togashi, *Angew. Chem.* **2004**, *116*, 4400–4402; *Angew. Chem. Int. Ed.* **2004**, *43*, 4300–4302; k) E. M. Nolan, S. J. Lippard, *J. Am. Chem. Soc.* **2003**, *125*, 14270–14271.

[18] P. L. McGrier, K. M. Solntsev, J. Schönhaber, S. M. Brombosz, L. M. Tolbert, U. H. F. Bunz, *Chem. Commun.* **2007**, 2127–2129.

[19] a) E. Negishi, L. Anastasia, *Chem. Rev.* **2003**, *103*, 1979–2017; b) K. Sonogashira, *J. Organomet. Chem.* **2002**, *653*, 46–49; c) U. H. F. Bunz, *Chem. Rev.* **2000**, *100*, 1605–1645.
[20] a) K. M. Solntsev, D. Huppert, L. M. Tolbert, N. Agmon, *J. Am. Chem. Soc.* **1998**, *120*, 7981–7982; b) K. M. Solntsev, D. Huppert, N. Agmon, *J. Phys. Chem. A* **1998**, *102*, 9599–9606; c) K. M. Solntsev, D. Huppert, N. Agmon, *J. Phys. Chem. A* **1999**, *103*, 6984–6997.
[21] M. J. Kamlet, J.-L. M. Abboud, M. H. Abraham, R. W. Taft, *J. Org. Chem.* **1983**, *48*, 2877–2887.
[22] a) L. M. Tolbert, K. M. Solntsev, *Acc. Chem. Res.* **2002**, *35*, 19–27; b) R. A. Binstead, A. D. Zuberbühler, B. Jung, SPECIFIT version 3.0.40, Spectrum Software Associates, Marlborough, MA, **2007**.
[23] a) N. P. Slabbert, *Tetrahedron* **1977**, *33*, 821–824; b) F. Z. Erdemgil, S. Sanli, N. Sanli, G. Oezkan, J. Barbosa, J. Guiteras, J. L. Beltran, *Talanta* **2007**, *72*, 489–496.
[24] A. Weller, *Prog. React. Kinet.* **1961**, *1*, 189–214.
[25] N. K. Zaitsev, A. B. Demyashkevich, M. G. Kuzmin, *High Energy Chem.* **1980**, *14*, 116–120.
[26] The Contrast Colour Analyzer program is freeware and can be downloaded from http://www.visionaustralia.org.au/info.aspx?page=628.
[27] a) R. G. Brereton in *Chemometrics: Data Analysis for the Laboratory and Chemical Plant*, Wiley, New York, **2003**; b) K. J. Albert, N. S. Lewis, C. L. Schauer, G. A. Sotzing, S. E. Stitzel, T. P. Vaid, D. R. Walt, *Chem. Rev.* **2000**, *100*, 2595–2626.

Received: February 17, 2008
Published online: April 18, 2008

